NANO LETTERS

Subscriber access provided by OXFORD UNIV LIBR SVCS

Letter

Unexpected Benefits of Rapid Growth Rate for III#V Nanowires

Hannah J. Joyce, Qiang Gao, H. Hoe Tan, Chennupati Jagadish, Yong Kim, Melodie A. Fickenscher, Saranga Perera, Thang Ba Hoang, Leigh M. Smith, Howard E. Jackson, Jan M. Yarrison-Rice, Xin Zhang, and Jin Zou

Nano Lett., **2009**, 9 (2), 695-701• DOI: 10.1021/nl803182c • Publication Date (Web): 30 December 2008

Downloaded from http://pubs.acs.org on March 19, 2009

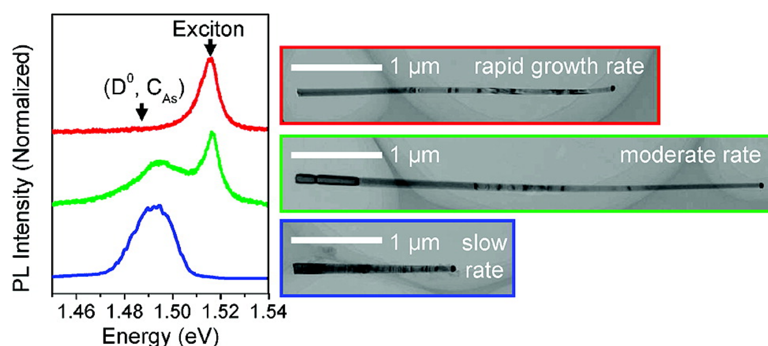

More About This Article

Additional resources and features associated with this article are available within the HTML version:

- Supporting Information
- Access to high resolution figures
- Links to articles and content related to this article
- Copyright permission to reproduce figures and/or text from this article

View the Full Text HTML

ACS Publications
High quality. High impact.

Nano Letters is published by the American Chemical Society. 1155 Sixteenth Street N.W., Washington, DC 20036

NANO LETTERS

2009
Vol. 9, No. 2
695-701

Unexpected Benefits of Rapid Growth Rate for III−V Nanowires

Hannah J. Joyce,[*,†] Qiang Gao,[†] H. Hoe Tan,[†] Chennupati Jagadish,[†] Yong Kim,[‡] Melodie A. Fickenscher,[§] Saranga Perera,[§] Thang Ba Hoang,[§] Leigh M. Smith,[§] Howard E. Jackson,[§] Jan M. Yarrison-Rice,[||] Xin Zhang,[⊥] and Jin Zou[⊥]

Department of Electronic Materials Engineering, Research School of Physics and Engineering, The Australian National University, Canberra, ACT 0200, Australia, Department of Physics, College of Natural Sciences, Dong-A University, Hadan 840, Sahagu, Busan 604-714, Korea, Department of Physics, University of Cincinnati, Cincinnati, Ohio Ohio 45221, Department of Physics, Miami University, Oxford, Ohio 45056, and School of Engineering and Centre for Microscopy and Microanalysis, The University of Queensland, St Lucia, QLD 4072, Australia

Received October 21, 2008; Revised Manuscript Received December 4, 2008

ABSTRACT

In conventional planar growth of bulk III−V materials, a slow growth rate favors high crystallographic quality, optical quality, and purity of the resulting material. Surprisingly, we observe exactly the opposite effect for Au-assisted GaAs nanowire growth. By employing a rapid growth rate, the resulting nanowires are markedly less tapered, are free of planar crystallographic defects, and have very high purity with minimal intrinsic dopant incorporation. Importantly, carrier lifetimes are not adversely affected. These results reveal intriguing behavior in the growth of nanoscale materials, and represent a significant advance toward the rational growth of nanowires for device applications.

Semiconductor nanowires have outstanding potential as nanocomponents of future devices and systems. In the past decade, several nanowire-based electronic and photonic devices have been demonstrated, including solar cells,[1] lasers,[2] light-emitting diodes,[3] photodetectors,[4] biosensors,[5] and transistors for ultrahigh density logic and memory devices.[6] Among semiconductor nanowires, III−V nanowires show particular promise due to the superior electrical and optical properties of III−V materials.[7] For example, the GaAs materials system features a direct band gap and high electron mobility. This makes GaAs nanowires prime candidates for future optoelectronic devices,[8] just as GaAs bulk materials and associated heterostructures are currently of great importance in the optoelectronics industry. Furthermore, III−V nanowires can be integrated with existing Si microelectronics technology.[9]

The development of III−V nanowire-based devices depends on the ability to fabricate nanowires with tight control over properties such as morphology, crystal structure, and composition. The challenge is to produce nanowires free of crystallographic defects with uniform diameters and with high purity. Perhaps the most promising and most common growth technique for III−V nanowires is metalorganic chemical vapor deposition (MOCVD) using Au nanoparticles as catalysts, via a vapor−liquid−solid (VLS)[10] or vapor−solid−solid (VSS) mechanism.[7] This approach offers great flexibility and high accuracy and is readily scalable for industrial mass fabrication. A number of growth parameters can be tailored for optimal nanowire growth: growth temperature,[11,12] the input V/III ratio,[12−14] and the absolute flow rates of group III and group V precursor species.

Increasing the absolute group III and group V flow rates directly increases the nanowire growth rate.[15,16] There are however, only limited reports of the effects of III and V flow rates on essential nanowire properties, such as crystallographic quality, optical properties, and compositional purity. In this letter, we investigate how the absolute precursor flow rates, or equivalently the nanowire growth rate, can be chosen to tailor nanowire properties.

In conventional planar epitaxy of bulk materials, a rapid growth rate is associated with lower quality material. The same would be assumed for nanowires.[17] We find, unexpectedly, the opposite result; a rapid nanowire growth rate can significantly improve nanowire properties. First, nanowires grown at a rapid rate exhibit very uniform, minimally tapered morphologies. This reduced tapering is especially desirable for devices such as nanowire lasers, where a uniform

* To whom correspondence should be addressed. E-mail: hjj109@rsphysse.anu.edu.au.
[†] The Australian National University.
[‡] Dong-A University.
[§] University of Cincinnati.
[||] Miami University
[⊥] The University of Queensland.

10.1021/nl803182c CCC: $40.75 © 2009 American Chemical Society
Published on Web 12/30/2008

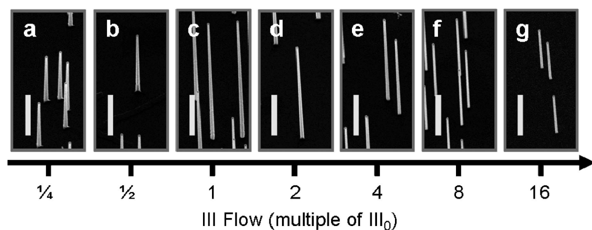

Figure 1. FESEM images of nanowires grown at constant V/III ratio of 46 and the indicated III flows: (a) III = 1/4 III_0, t = 60 min, (b) III = 1/2 III_0, t = 30 min, (c) III = III_0, t = 15 min, (d) III = 2 III_0, t = 7.5 min, (e) III = 4 III_0, t = 225 s (f) III = 8 III_0, t = 112.5 s and (g) III = 16 III_0, t = 56.25 s. Axis is logarithmic. Samples are tilted at 40°. Scale bars are 1 μm.

nanowire diameter should enhance the nanowire's performance as a resonant cavity. Second, transmission electron microscopy (TEM) investigations reveal that a high growth rate eliminates planar crystallographic defects. Photoluminescence (PL) measurements on these nanowires reveal strong excitonic emission with minimal impurity-related emission, indicating their high purity. Significantly, increasing nanowire growth rate has no adverse effect on exciton lifetime, and consequently nanowire quantum efficiency is not compromised. For these reasons, rapid growth rates are recommended for high quality III−V nanowires. We explain these unexpected results with reference to previous studies of nanowire and bulk epitaxy.

In this study, GaAs nanowires were grown on semi-insulating GaAs (111)B substrates using trimethylgallium (TMG) and AsH_3 precursors. GaAs(111)B substrates were treated with poly-L-lysine (PLL) solution, and a solution of colloidal 50 nm diameter Au nanoparticles, as described in previous reports.[11,14] Nanowires, catalyzed by these nanoparticles, were grown by horizontal flow MOCVD at a pressure of 100 mbar and a total gas flow rate of 15 slm. Prior to growth the substrate was annealed in situ at 600 °C under AsH_3 ambient to desorb surface contaminants. After cooling to a growth temperature of 450 °C, TMG was introduced to initiate nanowire growth.

The control, or standard, group III (TMG) and group V (AsH_3) flow rates were $III_0 = 1.2 \times 10^{-5}$ mol/min and $V_0 = 5.4 \times 10^{-4}$ mol/min, respectively and the V/III ratio was 46. For other growths, III_0 and V_0 were scaled by factors of 1/4, 1/2, 1, 2, 4, 8, and 16 to span flow ranges of III = 2.9×10^{-6} to 1.9×10^{-4} mol/min and V = 1.3×10^{-4} to 8.6×10^{-3} mol/min. Group III and group V flows were scaled equally, so that V/III ratio remained at 46. Throughout this letter, III and V flows will be expressed as multiples of III_0 and V_0, respectively. For nanowire samples grown with III = III_0, growth time (t) was 15 min. For other samples, growth time was scaled inversely with group III flow. This was to achieve nanowires of reasonable height, between 2 and 5 μm, across all samples.

Adjunct studies were performed at different V/III ratios of 12, 23, and 93.

First, we note that precursor flow rates have profound effects on nanowire morphology. Figure 1 illustrates field emission scanning electron microscope (FESEM, Hitachi

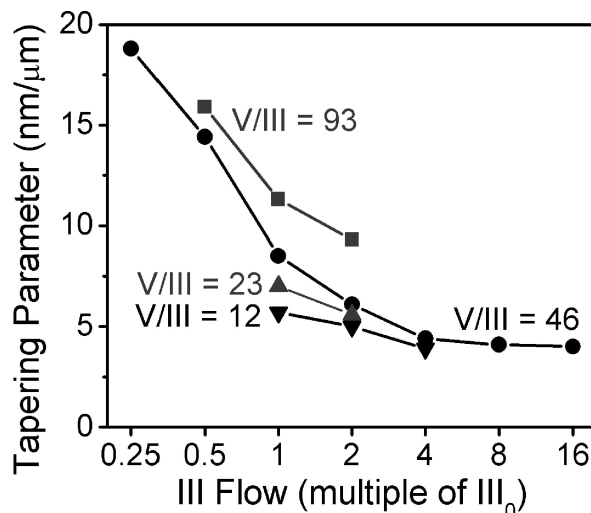

Figure 2. Tapering parameter versus precursor flow rate. Straight lines group data sets for a constant V/III ratio. Abscissa scale is logarithmic. The tapering parameter, $\Delta r/\Delta l$, was determined at approximately 1 μm intervals along the length of each nanowire, then averaged for each nanowire. Each data point represents an overall average from at least 5 nanowires. Standard deviations for each data point were less than 3 nm/μm.

S4500 operated at an accelerating voltage of 3 kV) images of GaAs nanowires grown at different growth rates and V/III of 46. The nanowires grow epitaxially in the [111]B direction normal to the substrate surface.

Au-assisted [111]B nanowire growth is termed "axial growth". Broadly speaking, the axial nanowire growth rate increases with increasing III and V flow, although the relationship is not perfectly linear. This has been addressed in previous work[10,15,16] and in the Supporting Information, so will not be considered in detail here.

Thin layer growth on nanowire sidewalls is termed "radial growth". Tapered nanowire morphologies, whereby nanowires exhibit wider bases and taper to narrower Au-capped tips, are a consequence of radial growth. The nanowire bases receive a greater fraction of precursor materials diffusing from the substrate,[16] and are exposed to reaction species longer than the more recently grown Au-capped tip. Like the axial growth rate, the radial growth rate too increases with III and V flow.[16]

Yet, inspecting Figure 1, nanowires grown at high III and V flow rates appear least tapered. To quantify tapering, we define the tapering parameter as the increase in nanowire radius, Δr, per unit nanowire length, Δl. This is equivalent to the ratio of radial (R_{radial}) to axial (R_{axial}) growth rates

$$\text{tapering parameter} = \frac{\Delta r}{\Delta l} = \frac{R_{radial}}{R_{axial}}$$

In Figure 2, the tapering parameter is plotted versus precursor flow rates. The figure includes data from the adjunct studies, each performed at a constant V/III ratio. Undoubtedly, tapering is reduced by increasing precursor flow.

To explain this finding, we note that axial growth is mass transport limited.[15,18] Therefore R_{axial} increases significantly

with increasing precursor flow rates. In contrast, radial growth is a thermally activated process, that is, kinetically limited.[18,19] Therefore the R_{radial} is strongly affected by growth temperature and is affected less significantly by precursor flow rates. Because R_{axial} increases significantly and R_{radial} increases only marginally, high precursor flow rates reduce nanowire tapering.

Therefore high V and III flows, which accordingly allows a short growth time to achieve a given nanowire length, produce minimally tapered nanowires. This is great advantage for laser applications which require uniform nanowire diameters. This is also potentially advantageous for ternary nanowires such as InGaAs[20] and AlGaAs.[21] One problem facing ternary nanowire growth is the spontaneous formation of a core−shell structure, where radial growth forms a shell of a different composition to the axially grown nanowire core.[21] By reducing the amount of radial growth, high precursor flows coupled with short growth times, may prevent spontaneous shell structures and achieve compositional uniformity in ternary nanowires.

We now consider nanowire crystallographic properties as a function of III and V flow. For TEM investigations, nanowires were dispersed onto holey carbon grids and these specimens were examined using a FEI Tecnai F30. To simplify discussion we occasionally use the phrase "increasing (decreasing) growth rate" to describe increasing (decreasing) III and V flow rate while keeping V/III ratio constant.

Crystallographic imperfections can limit the performance of nanowire devices. Unfortunately, the phase purity of [111]B-oriented III−V nanowires is difficult to control. Nanowires can be wurtzite structure[22] or zinc-blende structure[23,24] and generally feature multiple stacking faults or twin defects.[23,24] These defects significantly alter the optical and electronic properties of III−V nanowires.[25]

In this study, all GaAs nanowires were of zinc blende crystal structure, the stable bulk phase. Twin defects were identified by tilting each nanowire to the [110] zone axis. Figure 3a illustrates a TEM image of a twinned nanowire grown at a slow growth rate (III = 1/4 III_0, V = 1/4 V_0). Intriguingly, the nanowire of Figure 3b, grown at a high growth rate (III = 4 III_0, V = 4 V_0) is completely twin free. In Figure 3c, we plot twin density against precursor flow rate. We define twin density as the number of twin defects per unit (micrometer) of nanowire length. Each data point of Figure 3c is averaged over at least 3 nanowires. At the higher growth rates (above III = 4 III_0, V = 4 V_0), all nanowires examined were twin free and this data could not be plotted on the logarithmic axis of Figure 3c. Clearly, increasing both precursor flows, and consequently increasing growth rate, decreases the twin density.

This is an unexpected result. Increasing precursor flows increases the supersaturation of the vapor and liquid phases. According to theoretical and experimental studies of both planar and nanowire growth, a higher supersaturation (or supercooling) causes twin defects,[26−28] and can even drive wurtzite nanowire growth.[28−30] Note that a wurtzite structure is equivalent to a zinc blende structure with a twin plane every alternate monolayer.

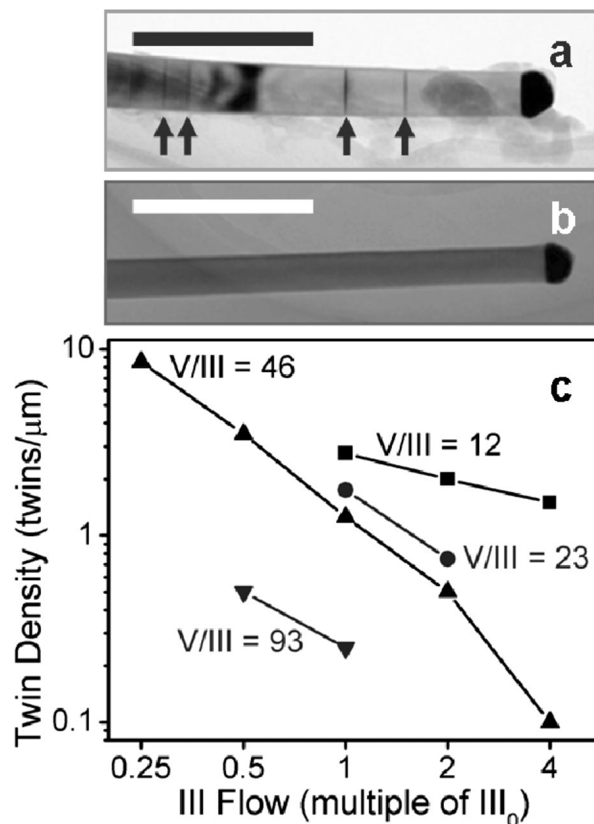

Figure 3. (a,b) TEM images of (a) a twinned nanowire grown with a slow growth rate (III = 1/4 III_0, V = 1/4 V_0) and (b) a twin-free nanowire grown at a rapid growth rate (III = 4 III_0, V = 4 V_0). Arrows indicate twin defects. Scale bar is 250 nm. (c) Twin density versus III flow. Group III flows are expressed as multiples of III_0. Straight lines group data sets for a constant V/III ratio. Axes are logarithmic.

One possible explanation for this unexpected result is outlined below. This explanation concerns surface and interfacial tensions, which reportedly drive twin formation in several nanowire[31,32] and bulk systems.[26] During nanowire growth, each plane nucleates at the triple phase line where nanowire, nanoparticle, and the ambient atmosphere meet.[23,30] Twin planes, too, nucleate at this triple phase line.[23] Several processes take place continuously during nanowire growth: nanowire side facets form, the shape and wettability of the nanoparticle−nanowire interface can change, and the nanoparticle can deform to wet this interface.[23,32,33] Fluctuations in mass transport and thermal fluctuations can also occur.[23,34] Consequently surface and interfacial tensions at the triple phase line can change dynamically throughout growth.[34] Twin plane nucleation is believed to relieve these surface and interfacial tensions, when these tensions exceed critical values.[31,32]

We propose that As and Ga precursor species act to reduce these surface and interfacial tensions. Arsenic species have low solubility in Au[35] and are thought to behave as surfactants when adsorbed on the Au nanoparticle surface.[36] For example, when the arsenic species $AsCl_3$ is added during Au-assisted VLS growth of Ge wires, the $AsCl_3$ acts as a surfactant on the Au droplet surface. Thus it decreases both the vapor−liquid and liquid−solid surface energies in the

Au droplet−Ge wire system.[34] Furthermore, in melt growth of bulk GaAs material, the addition of excess arsenic is known to lower the surface tension of the melt, and thus suppresses twinning.[26] We expect that in the Au nanoparticle−GaAs system under study, arsenic species significantly lower the surface tension at the Au liquid−vapor interface. Arsenic species may also lower the interfacial energy at the Au liquid−GaAs nanowire interface, but this effect is expected to be less significant due to the rapid consumption of any arsenic surfactant species present at this growth interface, into new nanowire growth.[14]

On the other hand, Ga dissolves into the nanoparticle to make it more Ga rich. Ga has lower surface and interfacial energies than pure Au,[37] so we expect a higher Ga concentration would reduce the nanoparticle surface and interfacial tensions.[30,38] Thus, both As and Ga species act to reduce surface and interface tensions throughout growth, so that the critical tensions for twin plane formation are exceeded less frequently. This may be responsible for the reduction in twin defects when As and Ga precursor flow rates are high.

In Figure 3c, we plotted lines connecting data points with common V/III ratios. In Figure S3 (Supporting Information), we again plot twin density against III flow, but this time plot lines to connect data points with common group V flow rates, rather than common V/III ratios. Interestingly, there is no clear trend in Figure S3 (Supporting Information). Increasing group III flow, while keeping group V flow constant, neither consistently promotes nor consistently hinders twin formation. We believe there are two opposing mechanisms that contribute to this result. At higher group III flows, the high supersaturation and rapid growth rate may indeed promote twin formation.[26−30] In opposition, the abundance of Ga species would decrease the surface and interfacial tensions of the nanoparticle−nanowire system, and hence hinder twin defect formation as argued above. Clearly, increasing group III flow alone is not sufficient to prevent twin formation. Group V flows must also be scaled up to significantly reduce twin density.[14]

Because GaAs nanowires offer the greatest potential in optoelectronics, their optical properties are of great importance. We use low temperature time integrated and time-resolved photoluminescence (PL) measurements to study the optical properties of these GaAs nanowires. For these PL measurements, GaAs nanowire cores were grown as described above, then clad in an AlGaAs shell to passivate the GaAs surface.[39,40] AlGaAs shell growth was performed for 20 min at 650 °C producing a shell approximately 30 nm thick with a nominal Al composition of 26%.

AlGaAs clad nanowires were transferred from the as-grown GaAs substrate to Si substrates by gently touching the two substrates together. Measurements were conducted at 18 K using slit confocal microphotoluminescence spectroscopy.[41] For time integrated PL spectra, ensembles of 5 to 10 nanowires were excited at 780 nm with a continuous wave Ti:sapphire laser defocused to an approximately 10 μm diameter spot. Time integrated PL was detected by a 2000 × 800 pixel liquid nitrogen-cooled CCD detector. Time-resolved PL measurements were performed on single isolated nanowires using time-correlated single photon counting. This employed pulsed laser excitation (780 nm, 800 μW) with 200 fs pulses at a 76 MHz repetition rate and a silicon avalanche photodiode detector. The temporal system response was measured to be 80 ps.

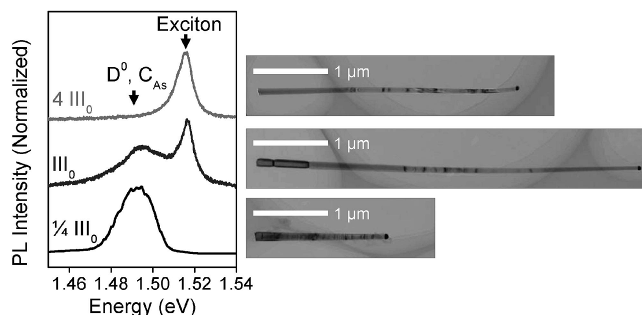

Figure 4. Normalized PL spectra comparing the relative magnitudes of DAP and exciton emission from nanowire ensembles grown with various III flows and a constant V/III ratio of 46. Spectra are offset for clarity. TEM images of the corresponding GaAs cores are illustrated alongside each spectrum.

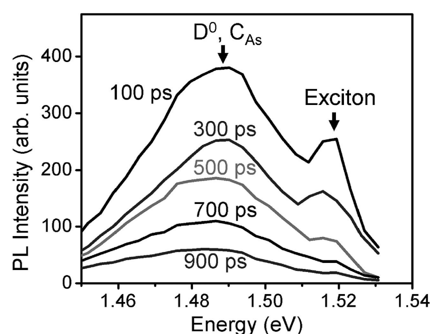

Figure 5. PL spectra at 100, 300, 500, 700, and 900 ps after the excitation laser pulse. Each spectrum is integrated over a 200 ps time window.

In Figure 4, we plot normalized PL spectra from three different nanowire samples. The peak at approximately 1.518 eV is attributed to free exciton recombination, as observed in bulk GaAs.[40,42] The lower energy peak between 1.48 and 1.50 eV is attributed to donor−acceptor pair (DAP) recombination involving a neutral donor and a carbon acceptor (D^0, C_{As}).[14,43] Note that the exciton peak is not evident in spectrum of the 1/4 III_0 sample in Figure 4, because this time integrated spectrum is dominated by the DAP peak. The time-resolved spectrum (Figure 5), on the other hand, shows the exciton peak at early times clearly.

Carbon has previously been identified as the dominant impurity in GaAs nanowires.[14,44] Carbon is the only impurity intrinsic to the MOCVD growth process.[45] It is a byproduct of the decomposition of the organometallic precursors, for example TMG.[45−47] Other contaminants, such as Si and Zn, are eliminated through the use of high purity sources. Consequently, controlling intrinsic C doping is a major concern in III−V nanowire growth. By careful choice of growth parameters, we can indeed minimize intrinsic C doping, as we now discuss.

The relative intensity of the DAP peak to the exciton peak indicates the degree of carbon impurity content.[46,48] We

Table 1. Exciton Lifetimes for Nanowires Grown with Different Growth Rates[a]

group III flow (multiple of III_0)	group V flow (multiple of V_0)	growth rate	exciton lifetime (ps)
1/4 III_0	1/4 V_0	slow	210
III_0	V_0	intermediate	200
4 III_0	4 V_0	rapid	190

[a] V/III ratio was held constant at 46.

compare the exciton and DAP peaks for nanowires grown with various growth rates (III = 1/4 III_0, III_0 and 4 III_0). The spectra of Figure 4 were obtained under low excitation power (90 μW) to avoid saturation of the DAP peak. In Figure 4, we note that the DAP peak intensity decreases with increasing growth rate. This indicates that the carbon impurity concentration decreases as growth rate increases. Apparently, a high growth rate favors high purity nanowires with minimal carbon contamination. This experiment was performed under conditions of constant V/III ratio (Figure 4). Under conditions of constant group V flow, exactly the same result holds (see Supporting Information, Figure S4). This again is surprising. A high growth rate is generally associated with lower quality growth and greater impurity incorporation.[49]

By examining Figure 4 we also note the large change in nanowire morphology concomitant with the change in C incorporation. With lower growth rates nanowires are more tapered, and have more C impurity incorporation. A likely explanation is that C incorporates preferentially via radial growth on the nanowire sidewalls. C has low solubility in Au,[50] so only a small amount of C is likely to be incorporated into the nanowire interior via Au-assisted axial growth. In contrast, C can be readily incorporated onto the nanowire sidewalls via the vapor−solid radial growth mechanism. Thus, nanowires with a greater proportion of radial growth (more tapered nanowires) have a greater degree of C incorporation. This same mechanism has been used to explain the formation of a boron- or phosphorus-rich shell in deliberately B- or P-doped Ge nanowires.[51]

Finally, we used time-resolved PL to probe the dynamics of photoexcited carriers in nanowires. Exciton lifetimes indicate the quality of the crystal and the presence of nonradiative recombination centers. These lifetimes were measured from the time decays of the exciton emission (at 1.518 eV).

Under the pulsed excitation used for the time-resolved measurements, all samples exhibited an exciton peak. We consider the sample (III = 1/4 III_0) corresponding to the bottommost time-integrated spectrum of Figure 4. Figure 5 illustrates time-resolved PL spectra from this sample displayed for consecutive 200 ps intervals after the excitation laser pulse. The exciton peak is clearly observed at early times after the excitation pulse (spectra at 100 and 300 ps), when the electron−hole density is highest. As the carriers recombine, the exciton peak rapidly decreases in intensity, leaving the lower energy DAP peak at later times (spectra at 500, 700, and 900 ps).

Exciton lifetimes for nanowires grown with slow, intermediate, and rapid growth rates are summarized in Table 1 (corresponding plots provided in the Supporting Information, Figure S5a). The exciton lifetimes are approximately 200 ps regardless of the growth rate. Increasing growth rate had no appreciable effect on exciton lifetime.

Table 2. Exciton Lifetimes for Nanowires Grown with Different V/III Ratios[a]

V/III ratio	exciton lifetime (ps)
12	280
46	200
93	120

[a] Group III flow was held constant at III_0.

This is contrasted with the pronounced effect seen upon increasing V/III ratio (Table 2 with corresponding plots provided in the Supporting Information, Figure S5b). Nanowires grown at a high V/III ratio of 93 have an exciton lifetime over 50% shorter than nanowires grown at a low V/III ratio of 11. The short exciton lifetime for nanowires grown at higher V/III ratios is attributed to an increase in excess arsenic-related defects at high V/III ratios.[52,53] These defects are most likely As antisite defects (As_{Ga}). As interstitials (As_i), Ga vacancies (V_{Ga}) and the so-called EL2 defect consisting of a complex of an As_{Ga} defect and an As_i defect[54] are also possible. These are the dominant defects in GaAs material grown at low temperatures by conventional growth techniques.[52,55] These defects create deep levels that rapidly trap free carriers and act as a nonradiative recombination centers, thereby reducing the radiative lifetime.[53,55,56] A high V/III ratio does impart some significant advantages to nanowires,[14] but the associated decrease in radiative lifetime is undesirable for optoelectronics applications which require a longer carrier lifetime. In contrast, increasing the growth rate is a superior means of obtaining excellent quality nanowires without compromising the exciton lifetime.

The time-resolved measurements point to a further unexpected phenomenon. One might expect that twin defects act as nonradiative recombination centers.[41] Indeed, twin-free nanowires have been reported with very long, nearly intrinsic exciton lifetimes.[41] Yet our current study indicates that excess arsenic-related defects (As_{Ga}, As_i, V_{Ga}, or EL2) are also primary nonradiative recombination centers. Take, for example, the nanowires grown at high V/III ratio (Table 2). These feature short exciton lifetimes, yet have a very low twin density.[14] Furthermore, using a rapid growth rate minimizes twin defects but does not enhance the exciton lifetime (Table 1). Therefore, we suggest that both twin defects and point defects must be eliminated to significantly improve nanowire optical properties.

In conclusion, a high growth rate has clear advantages for III−V nanowires. A high growth rate is achieved by scaling up both group III and group V precursor flows. Nanowires grown with fast growth rates are minimally tapered with very uniform diameters. Surprisingly, twin defects are markedly

reduced by employing a rapid growth rate. In addition, a rapid growth rate minimizes carbon impurity incorporation. C impurities are thought to be incorporated preferentially into radial growth on the nanowire sidewalls, rather than via Au-assisted axial growth. Clearly, high growth rates impart excellent crystallographic and optical nanowire properties. Furthermore, these results should translate to other important III−V nanowire materials systems, and assist in producing high quality binary and ternary nanowires with device accessible properties.

Acknowledgment. We thank the Australian Research Council, the National Science Foundation (Grants ECCS-0701703 and DMR-0806700) and the Korean Science and Engineering Foundation (Grant F01-2007-000-10087-0) for financial support. HJJ thanks the Australian Research Council Nanotechnology Network for an overseas travel fellowship to enable her collaborative visit to the University of Cincinnati. The Australian National Fabrication Facility established under the Australian Government's National Collaborative Research Infrastructure Strategy, is gratefully acknowledged for providing access to the facilities used in this research.

Supporting Information Available: Figures S1−S5, and a discussion of the axial growth rate dependence on precursor flow. This material is available free of charge via the Internet at http://pubs.acs.org.

References

(1) Law, M.; Greene, L. E.; Johnson, J. C.; Saykally, R.; Yang, P. *Nat. Mater.* **2005**, *4*, 455–459.
(2) (a) Huang, M. H.; Mao, S.; Feick, H.; Yan, H.; Wu, Y.; Kind, H.; Weber, E.; Russo, R.; Yang, P. *Science* **2001**, *292*, 1897–1899. (b) Duan, X. F.; Huang, Y.; Agarwal, R.; Lieber, C. M. *Nature* **2003**, *421*, 241–245.
(3) Park, H.-G.; Barrelet, C. J.; Wu, Y.; Tian, B.; Qian, F.; Lieber, C. M. *Nat. Photon.* **2008**, *2*, 622–626.
(4) (a) Wang, J.; Gudiksen, M. S.; Duan, X.; Cui, Y.; Lieber, C. M. *Science* **2001**, *293*, 1455–7. (b) Gu, Y.; Kwak, E.-S.; Lensch, J. L.; Allen, J. E.; Odom, T. W.; Lauhon, L. J. *Appl. Phys. Lett.* **2005**, *87*, 043111. (c) Pettersson, H.; Trägårdh, J.; Persson, A. I.; Landin, L.; Hessman, D.; Samuelson, L. *Nano Lett.* **2006**, *6*, 229–232.
(5) Hahm, J.-I.; Lieber, C. M. *Nano Lett.* **2004**, *4*, 51–54.
(6) Ng, H. T.; Han, J.; Yamada, T.; Nguyen, P.; Chen, Y. P.; Meyyappan, M. *Nano Lett.* **2004**, *4*, 1247–1252.
(7) Dick, K. A.; Deppert, K.; Karlsson, L. S.; Wallenberg, L. R.; Samuelson, L.; Seifert, W. *Adv. Funct. Mater.* **2005**, *15*, 1603–1610.
(8) (a) Duan, X.; Wang, J.; Lieber, C. M. *Appl. Phys. Lett.* **2000**, *76*, 1116–1118. (b) Hua, B.; Motohisa, J.; Ding, Y.; Hara, S.; Fukui, T. *Appl. Phys. Lett.* **2007**, *91*, 131112.
(9) (a) Mårtensson, T.; Svensson, C. P. T.; Wacaser, B. A.; Larsson, M. W.; Seifert, W.; Deppert, K.; Gustafsson, A.; Wallenberg, L. R.; Samuelson, L. *Nano Lett.* **2004**, *4*, 1987–1990. (b) Yi, S. S.; Girolami, G.; Amano, J.; Islam, M. S.; Sharma, S.; Kamins, T. I.; Kimukin, I. *Appl. Phys. Lett.* **2006**, *89*, 133121. (c) Chuang, L. C.; Moewe, M.; Chase, C.; Kobayashi, N. P.; Chang-Hasnain, C.; Crankshaw, S. *Appl. Phys. Lett.* **2007**, *90*, 043115.
(10) Hiruma, K.; Yazawa, M.; Haraguchi, K.; Ogawa, K.; Katsuyama, T.; Koguchi, M.; Kakibayashi, H. *J. Appl. Phys.* **1993**, *74*, 3162–3171.
(11) Joyce, H. J.; Gao, Q.; Tan, H. H.; Jagadish, C.; Kim, Y.; Zhang, X.; Guo, Y.; Zou, J. *Nano Lett.* **2007**, *7*, 921–926.
(12) Dayeh, S. A.; Yu, E. T.; Wang, D. *Nano Lett.* **2007**, *7*, 2486–2490.
(13) Chuang, L. C.; Moewe, M.; Crankshaw, S.; Chang-Hasnain, C. *Appl. Phys. Lett.* **2008**, *92*, 013121.
(14) Joyce, H. J.; Gao, Q.; Tan, H. H.; Jagadish, C.; Kim, Y.; Fickenscher, M. A.; Perera, S.; Hoang, T. B.; Smith, L. M.; Jackson, H. E.; Yarrison-Rice, J. M.; Zhang, X.; Zou, J. *Adv. Funct. Mater.* **2008**, *18*, 3794–3800.
(15) Verheijen, M. A.; Immink, G.; de Smet, T.; Borgström, M. T.; Bakkers, E. P. A. M. *J. Am. Chem. Soc.* **2006**, *128*, 1353–1359.
(16) Dick, K. A.; Deppert, K.; Samuelson, L.; Seifert, W. *J. Cryst. Growth* **2006**, *297*, 326–333.
(17) Takahashi, K.; Moriizumi, T. *Jpn. J. Appl. Phys.* **1966**, *5*, 657–662.
(18) Johansson, J.; Svensson, C. P. T.; Mårtensson, T.; Samuelson, L.; Seifert, W. *J. Phys. Chem. B* **2005**, *109*, 13567–13571.
(19) Borgström, M.; Deppert, K.; Samuelson, L.; Seifert, W. *J. Cryst. Growth* **2004**, *260*, 18–22.
(20) Kim, Y.; Joyce, H. J.; Gao, Q.; Tan, H. H.; Jagadish, C.; Paladugu, M.; Zou, J.; Suvorova, A. A. *Nano Lett.* **2006**, *6*, 599–604.
(21) Lim, S. K.; Tambe, M. J.; Brewster, M. M.; Gradecak, S. *Nano Lett.* **2008**, *8*, 1386–1392.
(22) Koguchi, M.; Kakibayashi, H.; Yazawa, M.; Hiruma, K.; Katsuyama, T. *Jpn. J. Appl. Phys.* **1992**, *31*, 2061–2065.
(23) Johansson, J.; Karlsson, L. S.; Svensson, C. P. T.; Mårtensson, T.; Wacaser, B. A.; Deppert, K.; Samuelson, L.; Seifert, W. *Nat. Mater.* **2006**, *5*, 574–580.
(24) (a) Zou, J.; Paladugu, M.; Wang, H.; Auchterlonie, G. J.; Guo, Y.; Kim, Y.; Gao, Q.; Joyce, H. J.; Tan, H. H.; Jagadish, C. *Small* **2007**, *3*, 389–393. (b) Karlsson, L. S.; Dick, K. A.; Wagner, J. B.; Malm, J.-O.; Deppert, K.; Samuelson, L.; Wallenberg, L. R. *Nanotechnology* **2007**, 485717.
(25) (a) Mishra, A.; Titova, L. V.; Hoang, T. B.; Jackson, H. E.; Smith, L. M.; Yarrison-Rice, J. M.; Kim, Y.; Joyce, H. J.; Gao, Q.; Tan, H. H.; Jagadish, C. *Appl. Phys. Lett.* **2007**, *91*, 263104. (b) Bao, J.; Bell, D. C.; Capasso, F.; Wagner, J. B.; Mårtensson, T.; Trägårdh, J.; Samuelson, L. *Nano Lett.* **2008**, *8*, 836–841.
(26) Hurle, D. T. J. *J. Cryst. Growth* **1995**, *147*, 239–250.
(27) Hurle, D. T. J.; Rudolph, P. *J. Cryst. Growth* **2004**, *264*, 550–564.
(28) Johansson, J.; Karlsson, L. S.; Dick, K. A.; Bolinsson, J.; Wacaser, B. A.; Deppert, K.; Samuelson, L. *J. Cryst. Growth* **2008**, *310*, 5102–5105.
(29) Mandl, B.; Stangl, J.; Mårtensson, T.; Mikkelsen, A.; Eriksson, J.; Karlsson, L. S.; Bauer, G.; Samuelson, L.; Seifert, W. *Nano Lett.* **2006**, *6*, 1817–1821.
(30) Glas, F.; Harmand, J. C.; Patriarche, G. *Phys. Rev. Lett.* **2007**, *99*, 146101.
(31) Li, Q.; Gong, X.; Wang, C.; Wang, J.; Ip, K.; Hark, S. *Adv. Mater.* **2004**, *16*, 1436–1440.
(32) Hao, Y.; Meng, G.; Wang, Z. L.; Ye, C.; Zhang, L. *Nano Lett.* **2006**, *6*, 1650–1655.
(33) Ross, F. M.; Tersoff, J.; Reuter, M. C. *Phys. Rev. Lett.* **2005**, *95*, 146104.
(34) Givargizov, E. I. *J. Cryst. Growth* **1973**, *20*, 217–226.
(35) *Binary Alloy Phase Diagrams*, 1st ed.; Okamoto, H., Massalski, T. B., Eds.; ASM International: Metals Park, OH, 1986; Vol. 1, pp 191−192.
(36) Copel, M.; Reuter, M. C.; Kaxiras, E.; Tromp, R. M. *Phys. Rev. Lett.* **1989**, *63*, 632–635.
(37) Peng, H.; Meister, S.; Chan, C. K.; Zhang, X. F.; Cui, Y. *Nano Lett.* **2007**, *7*, 199–203.
(38) Song, M. S.; Jung, J. H.; Kim, Y.; Wang, Y.; Zou, J.; Joyce, H. J.; Gao, Q.; Tan, H. H.; Jagadish, C. *Nanotechnology* **2008**, 125602.
(39) Noborisaka, J.; Motohisa, J.; Hara, S.; Fukui, T. *Appl. Phys. Lett.* **2005**, *87*, 093109.
(40) Titova, L. V.; Hoang, T. B.; Jackson, H. E.; Smith, L. M.; Yarrison-Rice, J. M.; Kim, Y.; Joyce, H. J.; Tan, H. H.; Jagadish, C. *Appl. Phys. Lett.* **2006**, *89*, 173126.
(41) Perera, S.; Fickenscher, M. A.; Jackson, H. E.; Smith, L. M.; Yarrison-Rice, J. M.; Joyce, H. J.; Gao, Q.; Tan, H. H.; Jagadish, C.; Zhang, X.; Zou, J. *Appl. Phys. Lett.* **2008**, *93*, 053110.
(42) Swaminathan, V.; Haren, D. L. V.; Zilko, J. L.; Lu, P. Y.; Schumaker, N. E. *J. Appl. Phys.* **1985**, *57*, 5349–5353.
(43) (a) Skromme, B. J.; Low, T. S.; Roth, T. J.; Stillman, G. E.; Kennedy, J. K.; Abrokwah, J. K. *J. Electron. Mater.* **1983**, *12*, 433–457. (b) Skromme, B. J.; Stillman, G. E. *Phys. Rev. B* **1984**, *29*, 1982–1992.
(44) (a) Hiruma, K.; Yazawa, M.; Katsuyama, T.; Ogawa, K.; Haraguchi, K.; Koguchi, M.; Kakibayashi, H. *J. Appl. Phys.* **1995**, *77*, 447–462. (b) Mikkelsen, A.; Sköld, N.; Ouattara, L.; Lundgren, E. *Nanotechnology* **2006**, *17*, S362–S368.
(45) Dapkus, P. D.; Manasevit, H. M.; Hess, K. L.; Low, T. S.; Stillman, G. E. *J. Cryst. Growth* **1981**, *55*, 10–23.
(46) Kuech, T. F.; Veuhoff, E. *J. Cryst. Growth* **1984**, *68*, 148–156.
(47) Mori, H.; Takahashi, S. *Jpn. J. Appl. Phys.* **1984**, *23*, L877–L879.

(48) (a) Lu, Z. H.; Hanna, M. C.; Szmyd, D. M.; Oh, E. G.; Majerfeld, A. *Appl. Phys. Lett.* **1990**, *56*, 177–179. (b) Ciorga, M.; Bryja, L.; Misiewicz, J.; Paszkiewicz, R.; Panek, M.; Paszkiewicz, B.; Tlaczala, M. *Adv. Mater. Opt. Electron.* **1998**, *8*, 9–12.

(49) (a) Hall, R. N. *Phys. Rev.* **1952**, *88*, 139. (b) Hayakawa, Y.; Saitou, Y.; Sugimoto, Y.; Kumagawa, M. *J. Electron. Mater.* **1990**, *19*, 145–149.

(50) (a) Okamoto, H.; Massalski, T. *J. Phase Equilib.* **1984**, *5*, 378–379. (b) Takagi, D.; Kobayashi, Y.; Hibino, H.; Suzuki, S.; Homma, Y. *Nano Lett.* **2008**, *8*, 832–835.

(51) (a) Tutuc, E.; Appenzeller, J.; Reuter, M. C.; Guha, S. *Nano Lett.* **2006**, *6*, 2070–2074. (b) Tutuc, E.; Guha, S.; Chu, J. O. *Appl. Phys. Lett.* **2006**, *88*, 043113. (c) Tutuc, E.; Chu, J. O.; Ott, J. A.; Guha, S. *Appl. Phys. Lett.* **2006**, *89*, 263101.

(52) Liu, X.; Prasad, A.; Nishio, J.; Weber, E. R.; Liliental-Weber, Z.; Walukiewicz, W. *Appl. Phys. Lett.* **1995**, *67*, 279–281.

(53) (a) Ganikhanov, F.; Lin, G.-R.; Chen, W.-C.; Chang, C.-S.; Pan, C.-L. *Appl. Phys. Lett.* **1995**, *67*, 3465–3467. (b) Gregory, I. S.; Tey, C. M.; Cullis, A. G.; Evans, M. J.; Beere, H. E.; Farrer, I. *Phys. Rev. B* **2006**, *73*, 195201.

(54) Bourgoin, J. C.; Bardeleben, H. J. v.; Stiévenard, D. *J. Appl. Phys.* **1988**, *64*, R65–R92.

(55) Gupta, S.; Frankel, M. Y.; Valdmanis, J. A.; Whitaker, J. F.; Mourou, G. A.; Smith, F. W.; Calawa, A. R. *Appl. Phys. Lett.* **1991**, *59*, 3276–3278.

(56) (a) Martin, G. M.; Farges, J. P.; Jacob, G.; Hallais, J. P.; Poiblaud, G. *J. Appl. Phys.* **1980**, *51*, 2840–2852. (b) Eizenberg, M.; Hovel, H. J. *J. Appl. Phys.* **1991**, *69*, 2256–2263.

NL803182C